



ELSEVIER

www.elsevier.com/locate/ica

Inorganica Chimica Acta 325 (2001) 45–50

**Inorganica
Chimica Acta**

Synthesis and characterization of $\{[(\text{COD})\text{Rh}(\text{bis}-(2\text{R},3\text{R})-2,5\text{-diethylphospholanobenzene})]^+\text{BARF}^-\}$ for use in homogeneous catalysis in supercritical carbon dioxide

Bilgehan Guzel^{a,b}, Mohammad A. Omary^{a,c}, John P. Fackler Jr.^{a,*},
Aydin Akgerman^d

^a Laboratory for Molecular Structure and Bonding, Department of Chemistry, Texas A&M University, PO Box 300012, College Station, TX 77843-3012, USA

^b Kimya Bolumu, Cukurova University, 01330 Adana, Turkey

^c Department of Chemistry, University of North Texas, Denton, TX 76203, USA

^d Chemical Engineering Department, Texas A&M University, College Station, TX 77843-3122, USA

Received 19 June 2001; accepted 27 July 2001

Abstract

Reaction of $[(\text{COD})_2\text{Cl}_2\text{Rh}]$ (COD: *cyclo*-octadiene) with sodium tetrakis((3,5-trifluoromethyl)phenyl)borate (NaBARF) in the presence of an excess of COD yields $[(\text{COD})_2\text{Rh}]^+\text{BARF}^-$. The COD ligands are readily displaced by the bidentate ligand 1,2-bis((2R,5R)-2,5-diethylphosphalono)benzene (Et-DuPHOS) to form $[(\text{COD})\text{Rh}(\text{Et-DuPHOS})]\text{BARF}$, the structure of which has been determined by X-ray crystallography. BARF was selected as the counterion in order to achieve solubility in supercritical carbon dioxide for use in asymmetric hydrogenation and hydroformylation reactions. Density-functional theory calculations were used to study the intermediates in asymmetric hydroformylation of styrene. The energies of the two-enantiomer models differ by 11.3 kcal mol⁻¹. © 2001 Elsevier Science B.V. All rights reserved.

Keywords: Rhodium complexes; Phospholanes; Homogeneous catalysis; Supercritical fluids; Crystal structures

1. Introduction

Chiral rhodium phospholane complexes have found important applications as catalysts in hydroformylation and hydrogenation reactions. Hydroformylation is one of the most versatile methods for the functionalization of C=C bonds [1]. Numerous chiral phospholanes and phosphites have been synthesized to be used as ligands for transition-metal-catalyzed homogeneous asymmetric synthesis [2–5].

In recent years, there has been increasing interest in using supercritical carbon dioxide (scCO₂) as the reaction medium for organic synthesis [6,7]. Use of a supercritical reaction medium, in addition to being an environmentally benign solvent, has other advantages. Supercritical fluids have density tunable physicochemi-

cal properties affecting reaction rates and selectivities. The mass transfer characteristics are superior in comparison to liquid reaction media due to high diffusion coefficients and low viscosities. Finally, scCO₂ is inert to most reactions, it is non-toxic, non-flammable, readily available, inexpensive and has rather mild critical properties. Most homogeneous catalysts, however, are not soluble in scCO₂ without modification. It is well known that fluorine groups attached to ligands increase their solubility in scCO₂ [8]. Burk et al. [9] used Et-DuPHOS as a chiral bidentate ligand and prepared the $[(\text{COD})\text{Rh}(\text{Et-DuPHOS})]^+$ (COD: *cyclo*-octadiene) complex, with the counterion being either trifluoromethyl sulfonate or tetrakis(3,5-bis(trifluoromethyl)phenyl)borate (BARF). They reported that the solubility in scCO₂ of the complex with the BARF counterion at 40 °C and 5000 psia was 0.030 mM.

In this study, we report the synthesis and structural characterization of $[(\text{COD})\text{Rh}(\text{Et-DuPHOS})]\text{BARF}$.

* Corresponding author. Tel.: +1-979-845 2835; fax: +1-979-845 9351.

E-mail address: fackler@mail.chem.tamu.edu (J.P. Fackler, Jr.).

The synthesis follows a different synthetic route than that reported by Burk et al.

The BARF counterion renders the complex soluble in scCO_2 , which makes the catalysis suitable for homogeneous catalysis in scCO_2 . The structure of $[(\text{COD})\text{-Rh}(\text{Et-DuPHOS})]\text{BARF}$ is determined by single crystal X-ray crystallography for the first time. Density-functional theory (DFT) calculations are used to assess the use of the complex as an enantioselective catalyst for hydroformylation reactions.

2. Results and discussion

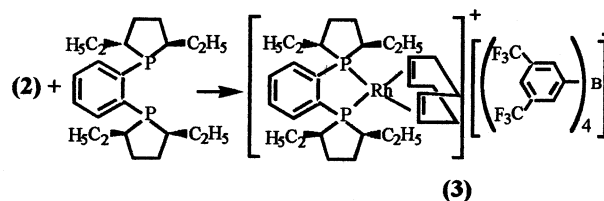
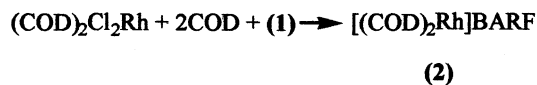
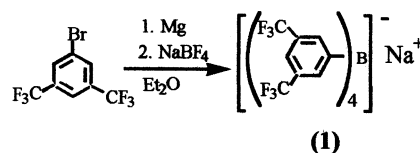
The general method of synthesis is given in Scheme 1. Analytical and spectroscopic data can be found in detail in Section 4.

2.1. $[(\text{COD})_2\text{Rh}]\text{BARF}$ (**2**)

^1H NMR (in CDCl_3) spectra show two peaks for the COD ligand at 2.4 ppm (CH_2) and 5.09 ppm (CH_2) and a multiplet for the aromatic protons in the BARF anion at 7.5 ppm. ^{19}F NMR spectra show a singlet at -62.08 ppm corresponding to the $-\text{CF}_3$ group in BARF [10]. Also consistent with the literature, the BARF anion has no co-ordination to the complex. The results of the elemental analysis of **2** are in agreement with the theoretical values.

2.2. $[(\text{COD})\text{Rh}(\text{Et-DuPHOS})]^+\text{BARF}$ (**3**)

Rhodium-phosphorus NMR coupling has been reviewed by several authors. The values are normally in the range of 81–150 Hz [11]. The peak at 69.7 ppm (d, $J_{\text{Rh-P}} = 147$ Hz) in the ^{31}P NMR spectra (in CDCl_3) is, therefore, consistent with the literature. The ^{19}F NMR spectra (in CDCl_3) show a singlet at -62.3 ppm. All the peaks obtained by ^1H NMR spectra were consistent with the literature [12]. The structure was determined by X-ray crystallography for crystals grown from a methylene chloride/hexane mixture (1:2). ORTEP drawings of **3** are shown in Figs. 1–3 for the $[(\text{COD})\text{Rh}(\text{Et-DuPHOS})]^+$ complex, the BARF counterion, and the whole compound, respectively. Selected bond lengths and angles are compiled in Table 1. The Rh–P, Rh–C and the COD C=C bond lengths, and the 85.4° P–Rh–P bond angle are all consistent with the literature [12]. The bond angles between the benzene ring and the phosphorous atoms, C–C–P(1A): 0124.8° and C–C–P(2A): 115.9° , indicate that the benzene ring has a 4.8° dihedral twist with respect to the P–Rh–P plane. The COD ligand is π -co-ordinated to Rh through the double bonded carbons. The bond angles indicate that two co-ordinated C atoms from COD are on the P–Rh–P plane. The other co-ordinated C atoms from



Scheme 1. Synthesis reaction of NaBARF, $[(\text{COD})_2\text{Rh}]\text{BARF}$ and $[(\text{COD})\text{Rh}(\text{Et-DuPHOS})]\text{BARF}$.

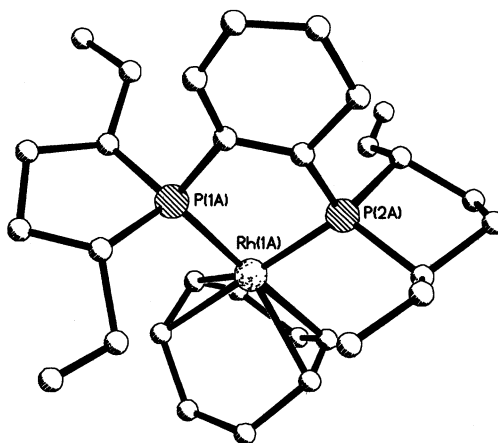


Fig. 1. ORTEP drawing of the $[(\text{COD})\text{Rh}(\text{Et-DuPHOS})]^+$ cation in **3** (50% probability).

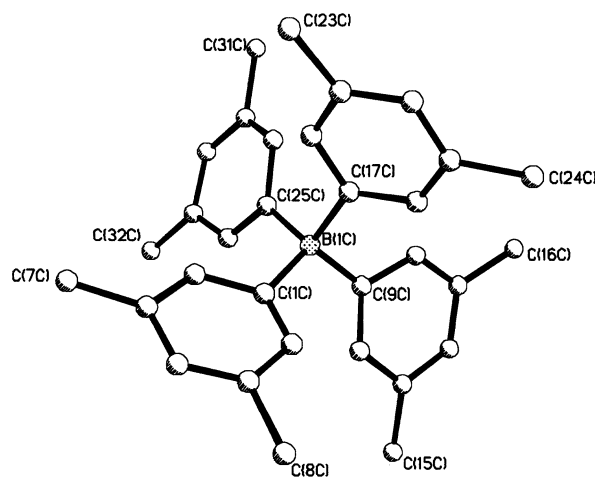


Fig. 2. ORTEP drawing of the BARF anion in **3** (50% probability). The fluorine atoms of the CF_3 groups are omitted for clarity.

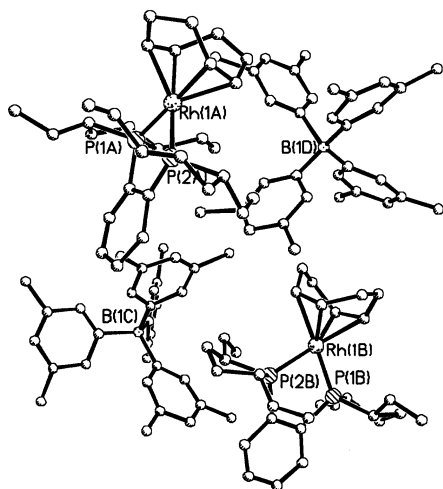


Fig. 3. ORTEP drawing of the crystal structure of **3** (50% probability). The fluorine atoms of the CF_3 groups are omitted for clarity.

Table 1
Selected interatomic distances (Å) and bond angles (°) for **3**

Bond distances

Rh(1A)–C(1A)	2.16(3)
Rh(1A)–C(8A)	2.35(3)
Rh(1A)–C(4A)	2.23(2)
Rh(1A)–C(5A)	2.24(2)
Rh(1A)–P(2A)	2.238(6)
Rh(1A)–P(1A)	2.275(5)
C(1A)–C(8A)	1.34(3)
C(4A)–C(5A)	1.39(3)
B(1C)–C(1C)	1.67(3)
B(1C)–C(9C)	1.59(3)
B(1C)–C(17C)	1.65(3)
B(1C)–C(25C)	1.66(3)

Bond angles

P(1A)–Rh(1A)–P(2A)	85.4(2)
P(1A)–Rh(1A)–C(8A)	94.1(6)
P(1A)–Rh(1A)–C(1A)	101.1(7)
P(1A)–Rh(1A)–C(4A)	178.4(7)
P(1A)–Rh(1A)–C(5A)	145.3(7)
P(2A)–Rh(1A)–C(4A)	93.9(7)
P(2A)–Rh(1A)–C(5A)	98.0(7)
P(2A)–Rh(1A)–C(8A)	176.1(7)
P(2A)–Rh(1A)–C(1A)	149.6(7)
C(4A)–Rh(1A)–C(8A)	86.6(9)
C(4A)–Rh(1A)–C(1A)	78.7(9)
C(5A)–Rh(1A)–C(8A)	80.2(9)
C(5A)–Rh(1A)–C(1A)	93.2(9)
C(14A)–C(9A)–P(1A)	124.8(19)
C(11A)–C(10A)–P(2A)	115.9(16)
C(9C)–B(1C)–C(1C)	111.3(16)
C(9C)–B(1C)–C(17C)	112.0(16)
C(9C)–B(1C)–C(25C)	104.1(17)
C(17C)–B(1C)–C(1C)	100.4(15)
C(25C)–B(1C)–C(1C)	115.7(17)
C(17C)–B(1C)–C(25C)	113.6(17)

COD form a 30° angle and one is above the P–Rh–P plane, whereas the other is below the plane. These data indicate that the complex has a square planar structure

and that the five-membered phospholane ring has a C_2 symmetry. The bond angles of the BARF anion presented in Table 1 indicate that it has a tetrahedral geometry.

3. Density-functional theory calculations

Calculations were performed for the molecular models shown in Fig. 4. The calculations were at the DFT

Table 2
Crystal data and refinement details for **3**

Chemical formula	$\text{C}_{62}\text{H}_{60}\text{BF}_{24}\text{P}_2\text{Rh}$
Formula weight	1436.76
Crystal system	monoclinic
Space group	$P2_1$
Temperature (K)	193
Wavelength (Å)	0.71073
Unit cell dimensions	
<i>a</i> (Å)	18.866(4)
<i>b</i> (Å)	13.322(5)
<i>c</i> (Å)	25.300(3)
β (°)	92.313(16)
<i>V</i> (Å ³)	6354(3)
<i>Z</i>	8
ρ_{calc} (mg m ⁻³)	3.004
μ (cm ⁻¹)	8.57
R_1^a [$I > 2\sigma(I)$]	0.0929
wR_2^b [$I > 2\sigma(I)$]	0.2228
R_1^a (all data)	0.1542
wR_2^b (all data)	0.2594

$$^a R_1 = \frac{\sum \|F_o\| - \|F_c\|}{\sum \|F_o\|}$$

$$^b wR_2 = \left\{ \frac{\sum [w(F_o^2 - F_c^2)^2]}{\sum [w(F_o^2)^2]} \right\}^{1/2}$$

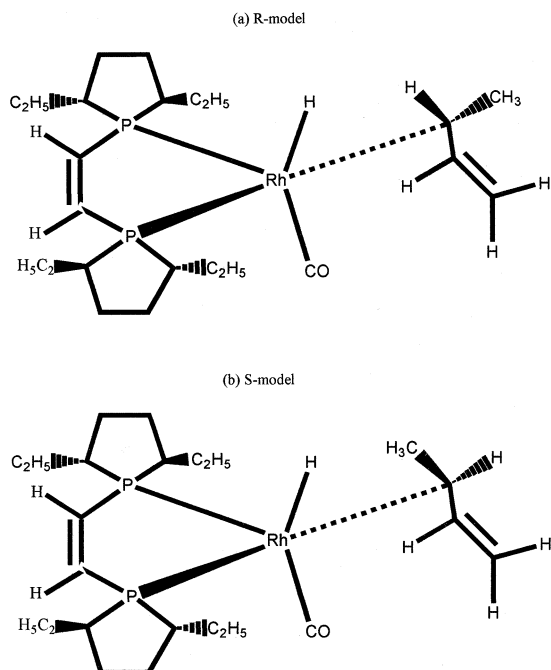


Fig. 4. Enantiomer models used in the DFT calculations.

level with a B3LYP formalism, as described in Section 6. The purpose of these calculations is to investigate enantioselectivity from the use of **3** as a catalyst for the hydroformylation of styrene, a reaction we have been pursuing experimentally. Enantioselectivity in hydroformylation reactions results from hydride insertion to yield two possible enantiomers, if the reaction follows textbook catalytic cycles [13]. With the benzene rings in the styrene substrate and the DuPHOS ligand, modeling the relevant intermediate in the catalytic cycle using modern DFT methods is not feasible. Instead of deferring to less reliable computational methods, such as molecular mechanics, we elected to pursue DFT calculations after simplifying the computational models by replacing the phenyl groups with vinyl groups. This simplification does not significantly affect the steric and electronic environments of the chiral centers in the intermediates. With this approach, the two enantiomers shown in Fig. 4 represent the proposed intermediates in the catalytic cycle of hydroformylation that would lead to the branched aldehyde. The results of the calculations indicate that the *R*-enantiomer is more stable than the *S*-enantiomer by 47.4 kJ mol⁻¹ (11.3 kcal mol⁻¹). This result suggests that the substrate ‘feels’ the chiral centers in the DuPHOS ligand. Therefore, if the hydroformylation of styrene is controlled by hydride insertion, the calculations predict an enantiomeric excess for the *R*-aldehyde. However, the calculations predict that enantioselectivity may not be feasible, if the rate determining step occurs prior to hydride insertion in the catalytic cycle (e.g., oxidative addition of H₂, addition of styrene to form the π-adduct). Further discussion of the relevance of this conclusion to our experimental results [14] on the hydroformylation of styrene in scCO₂ using **3** as catalyst, including mechanistic and kinetics data, will be published elsewhere. Consistent with our findings, there is evidence in the literature suggesting that the kinetics of hydroformylation using rhodium catalysts are different in scCO₂ from the kinetics in organic solvents [15].

4. Experimental

4.1. General

All synthetic procedures were carried out under a nitrogen atmosphere using standard Schlenk and glove box techniques, and using flame-dried glassware. Diethyl ether (Et₂O), hexane, and tetrahydrofuran (THF) were distilled from sodium benzophenone ketyl under nitrogen. Methylene chloride (CH₂Cl₂) was distilled from CaH₂. Preparation of the sodium salt of BARF was carried out (Scheme 1) as described by Brookhart et al. [16] and Nishida et al. [17] and the product was

used without recrystallization. *Caution: Safety precautions should be taken while preparing BARF or any other reactions involving the use of a Grignard reagent with fluorinated substrates. Fatal explosions have occurred with such procedures.* All other chemicals were of reagent grade quality and were used without further purification.

4.2. Synthesis of [bis-cyclo-octa-1,5-diene-rhodium(I)]⁺BARF⁻ {[COD]₂Rh}BARF⁻ (**2**)

Bis(cyclo-octa-1,5-diene)-μ,μ'-dichlorodirhodium (493 mg, 1 mmol) and cyclo-octa-1,5-diene (0.2 ml excess) were dissolved in methylene chloride (5 ml). A solution of NaBARF (1775 mg, 2 mmol) in methylene chloride (10 ml) was added dropwise to the stirred (25 °C) red solution. After addition was complete, the deep red solution was stirred for 20 min and filtered through anhydrous MgSO₄, to remove NaCl, and then added to hexane (60 ml) to give dark red crystals of **2** [18]. The product was filtered off under nitrogen and recrystallized from dichloromethane/hexane (1:2). Yield 1.08 g (91%). m.p. 164–167 °C (dec.). Elemental analysis: Calc. for C₄₈H₃₆BF₂₄Rh: C, 47.79; H, 3.01. Found: C, 48.11; H, 3.11. ¹H NMR (200 MHz, CDCl₃) 2.4 ppm (s, 8H, COD-CH₂), 5.09 ppm (s, 4H, COD-CH), 7.5 ppm (s, 12H, Ph); ¹⁹F NMR (300 MHz, CDCl₃) -62.08 ppm (s, 24F, Ph(CF₃)₃).

4.3. Synthesis of [(cyclo-octadiene)rhodium(I)(1,2-bis-((2*R*,5*R*)-2,5-diethylphospholano)benzene)]⁺BARF⁻ {[COD]Rh(Et-DuPHOS)}BARF⁻ (**3**)

A modification of the procedure reported by Burk et al., and Schrock and Osborn [19] was used for the preparation of **3**. A solution of [(COD)₂Rh]BARF (500 mg, 0.42 mmol) in 15 ml of THF at 25 °C was added dropwise to a solution of 1,2-bis((2*R*,5*R*)-2,5-diethylphospholano)benzene (153 mg, 0.42 mmol) in 8 ml of THF. The color of the solution turned from yellow to orange upon phosphine addition. The reaction was stirred for 15 min and after that the THF was removed under reduced pressure precipitating an orange-red crystalline product. The product was dissolved in methylene chloride (7 ml), and hexane (40 ml) was added slowly to crystallize the product as an orange crystalline solid: yield 374 mg (62%). ¹H NMR (300 MHz, CDCl₃) 0.8 ppm (t, 6H, CH₃), 0.95 ppm (t, 6H, CH₃), 1.1–1.5 ppm (m, 8H, CH₂), 1.6–1.9 ppm (m, 4H, CH-CH₂), 2.1 ppm (m, COD-CH₂), 2.2–2.7 (m, 12H, COD-CH₂ and CH-CH₂), 4.85 ppm (s, 2H, COD-CH), 5.5 ppm (s, 2H, COD-CH), 7.6–7.9 ppm (m, 16H, Ph-H); ³¹P NMR (300 MHz, CDCl₃) 69.7 ppm (J_{Rh-P} = 147 Hz); ¹⁹F NMR (300 MHz, CDCl₃) -62.3 ppm (s, 24F, Ph(CF₃)₃).

5. X-ray structure determination of **3**

Suitable crystals of **3** were obtained by slow evaporation of a methylene chloride/hexane (1:2) solution at 25 °C. The structure was determined using direct methods (SHELXS 86 (Sheldrick, 1985)). Details of the crystal data, parameters for data collection, the solution and refinement of the structure are given in Table 2.

6. Computational details

All calculations were performed with the Gaussian 98 suite of programs [20] for the molecular models in Fig. 4. The calculations were at the DFT level [21] using the Becke three parameter [22] hybrid exchange functional and the Lee et al. [23] correlation functional, B3LYP. A Huzinaga/Dunning basis set [24] of a double-zeta quality was used for carbon and hydrogen atoms. A double-zeta basis set plus one polarization function on the P atoms was used, in order to properly describe the hypervalent character of phosphorous compounds. A small-core effective core potential (ECP) developed by Hay and Wadt [25] was used for the rhodium atoms to represent the 28 core electrons ($1s^2 2s^2 2p^6 3s^2 3p^6 3d^{10}$) with a double-zeta basis set for the 17 outer electrons from the atomic $4s^2 4p^6 5s^2 4d^7$ shells. The ECP for rhodium incorporates two relativistic effects for the core electrons, mass velocity and Darwin, and thus represents the dominant relativistic contributions to the behavior of the outer electrons. Single point energy calculations were carried out on the model systems. All graphical manipulations to produce the models and Gaussian 98 input files were done using Cerius² [26]. The geometry of the Rh(DuPHOS) moiety was taken directly from the crystal structure of **3**. The force field in Cerius² was used to optimize the C=C and C–H bonds in the vinyl group replacing the benzene ring in DuPHOS and to optimize the geometry of the added ligands (CO, H, $H_2C=CH-CH(CH_3)-$). The overall geometry around rhodium was constrained to a trigonal bipyramidal arrangement in both the R- and S-models.

7. Supplementary material

A CIF file of the crystallographic data for the structure of **3**.

Acknowledgements

Support from the Robert A. Welch Foundation and the Texas A&M Office of the Vice President for Research are gratefully acknowledged.

References

- [1] N. Sakai, S. Mano, K. Nozaki, H. Takaya, *J. Am. Chem. Soc.* 115 (1993) 7033.
- [2] (a) M.J. Burk, *Acc. Chem. Res.* 33 (2000) 363; (b) H.A. Hoveyda, D.A. Evans, G.C. Fu, *Chem. Rev.* 93 (1993) 1307.
- [3] A. Borner, D. Heller, *Tetrahedron Lett.* 42 (2001) 223.
- [4] (a) N. Sakai, K. Nozaki, H. Takaya, *J. Chem. Soc., Chem. Commun.* (1994) 395; (b) K. Nozaki, N. Sakai, T. Nanno, T. Higashijima, S. Mano, T. Horiuchi, H. Takaya, *J. Am. Chem. Soc.* 119 (1997) 4413; (c) K. Nozaki, T. Hiyama, S. Kacker, I.T. Horvath, *Organometallics* 19 (2000) 2031.
- [5] E.A. Hauptman, S. Sabo-Etienne, P.S. White, M. Brookhart, J.M. Garner, P.J. Fagan, J.C. Calabrese, *J. Am. Chem. Soc.* 116 (1994) 8038.
- [6] (a) P.G. Jessop, W. Leitner (Eds.), *Chemical Synthesis using Supercritical Fluids*, VCH, Weinheim, 1999; (b) E. Dinjus, R. Fornika, M. Scholz, in: R. van Eldik, C.D. Hubbard (Eds.), *Chemistry under Extreme or Non-Classical Conditions*, Wiley, New York, 1996, p. 219; (c) D.A. Morgenstern, R.M. LeLacheur, D.K. Morita, S.L. Borkowsky, S. Feng, G.H. Brown, L. Luan, M.F. Gross, M.J. Burk, W. Tumas, in: P.T. Anastas, T.C. Williamson (Eds.), *Green Chemistry*, ACS Symp. Ser. 626, American Chemical Society, Washington, DC, 1996, p. 132.
- [7] (a) T. Ikariya, Y. Kayaki, *Catal. Surv. Jpn.* 4 (2000) 39; (b) P.G. Jessop, T. Ikariya, R. Noyori, *Chem. Rev.* 99 (1999) 475; (c) A. Baiker, *Chem. Rev.* 99 (1999) 453; (d) P.G. Jessop, T. Ikariya, R. Noyori, *Science* 269 (1995) 1065; (e) G. Kaupp, *Angew. Chem., Int. Ed. Engl.* 33 (1994) 1452.
- [8] J.M. DeSimone, Z. Guan, C.S. Elsbernd, *Science* (1992) 357.
- [9] M.J. Burk, S. Feng, F.M. Gross, W. Tumas, *J. Am. Chem. Soc.* 117 (1995) 8277.
- [10] S. Berge, S. Braun, H.O. Kalinowski, *NMR Spectroscopy of the Non-Metallic Elements*, Wiley, New York, 1991, p. 416.
- [11] R. Harris, B.E. Mann, *NMR in the Periodic Table*, Academic Press, London, 1978, pp. 249–255.
- [12] M.J. Burk, J.E. Feaster, W.A. Nugent, R.L. Harlow, *J. Am. Chem. Soc.* 115 (1993) 10125.
- [13] C. Elschenbroich, A. Salzer, *Organometallics: A Concise Introduction*, second ed., VCH, Weinheim, 1992, pp. 434–437.
- [14] B. Lin, *Environmentally Friendly Organic Synthesis in Supercritical Carbon Dioxide*, Ph.D. Thesis, Texas A&M University, 2000.
- [15] D.R. Palo, C. Erkey, *Ind. Eng. Chem. Res.* 38 (1999b) 3786.
- [16] M. Brookhart, B. Grant, A.F. Volpe, *Organometallics* 11 (1992) 3920.
- [17] H. Nishida, N. Takada, M. Yashimura, *Bull. Chem. Soc. Jpn.* 57 (1984) 2600.
- [18] (a) J. Chatt, L.M. Venazzi, *J. Am. Chem. Soc.* (1957) 4735; (b) M. Green, T.A. Kuc, S.H. Taylor, *J. Chem. Soc. A* (1971) 2334; (c) K.R. Dunbar, C.S. Haefner, C.E. Uzelmeier, A. Howard, *Inorg. Chim. Acta* 240 (1995) 527.
- [19] R.R. Schrock, J.A. Osborn, *J. Am. Chem. Soc.* 93 (1971) 2397.
- [20] M.J. Frisch, G.W. Trucks, H.B. Schlegel, G.E. Scuseria, M.A. Robb, J.R. Cheeseman, V.G. Zakrzewski, J.A. Montgomery, R.E. Stratmann, J.C. Burant, S. Dapprich, J.M. Millam, A.D. Daniels, K.N. Kudin, M.C. Strain, O. Farkas, J. Tomasi, V. Barone, M. Cossi, R. Cammi, B. Mennucci, C. Pomelli, C. Adamo, S. Clifford, J. Ochterski, G.A. Petersson, P.Y. Ayala, Q. Cui, K. Morokuma, D.K. Malick, A.D. Rabuck, K. Raghavachari, J.B. Foresman, J. Cioslowski, J.V. Ortiz, B.B. Stefanov, G. Liu, A. Liashenko, P. Piskorz, I. Komaromi, R.

- Gomperts, R.L. Martin, D.J. Fox, T. Keith, M.A. Al-Laham, C.Y. Peng, A. Nanayakkara, C. Gonzalez, M. Challacombe, P.M.W. Gill, B.G. Johnson, W. Chen, M.W. Wong, J.L. Andres, M. Head-Gordon, E.S. Replogle, J.A. Pople, Gaussian 98 (Revision A.7), Gaussian, Inc., Pittsburgh PA, 1998.
- [21] R.G. Parr, W. Yang, *Density-Functional Theory of Atoms and Molecules*, Oxford University Press, Oxford, 1989.
- [22] A.D. Becke, *J. Chem. Phys.* 98 (1993) 5648.
- [23] (a) C. Lee, W. Yang, R.G. Parr, *Phys. Rev. B* 37 (1988) 785; (b) B. Miehlich, A. Savin, H. Stoll, H. Preuss, *Chem. Phys. Lett.* 157 (1989) 200.
- [24] T.H. Dunning Jr., P.J. Hay, in: H.F. Schaefer III (Ed.), *Modern Theoretical Chemistry*, vol. 3, Plenum Press, New York, 1976, p. 1.
- [25] P.J. Hay, W.R. Wadt, *J. Chem. Phys.* 82 (1985) 270.
- [26] Cerius², Release 4.0, Molecular Simulations Inc., 1999.